Kansas Geological Survey

Development of an Interactive Integrated Groundwater Modeling and Geographic Information System for the Upper Arkansas River Corridor Study

Ming-Shu Tsou, Donald O. Whittemore, and Yun-Sheng Yu

Kansas Geological Survey Open-File Report 97-35
May 1997

GEOHYDROLOGY

The University of Kansas, Lawrence, KS 66047 Tel. (913) 864-3965

Table of Contents

List of Figures

List of Tables

I. INTRODUCTION

1.1 Statement of the Problem

The Arkansas River entering the western border of Kansas from Colorado is one of the most saline rivers in the United States. Figure 1.1 (Whittemore and Butler, 1997) shows a plot of sulfate concentration versus river discharge near Coolidge located in Kansas near the border. The sulfate concentration is extremely high with a maximum of 2500 mg/L at low discharge. The average discharge near Coolidge is about 5.72 m^3/sec (U.S.G.S. Water Resources Data-Kansas, 1995). There were many days with no flow in 1903, 1954, 1960. At the average discharge, the corresponding sulfate concentration would likely be higher than 2000 mg/L. Most of the saline water entering Kansas infiltrates from the river channel and irrigation diversions into the alluvial and Ogallala aquifers, referred to as the High Plains aquifer. The saline river water enters the aquifer and migrates outward and downward in the High Plains aquifer and pollutes many wells located in the area. Clearly, the saline river water is the main source of high sulfate concentration to the High Plains aquifer (Whittemore et al., 1996). However, the exact mechanism of the spreading of the saline water from the upper aquifer to the lower aquifer and the severity of the pollution is not well understood and needs investigation.

Through the years of groundwater development for irrigation and water supply, the shallow alluvial aquifer has been highly polluted with saline water containing a sulfate concentration averaging about 2000 mg/L. The recommended sulfate concentration limit for drinking water is 250 mg/L. Because the upper aquifer contains saline water,

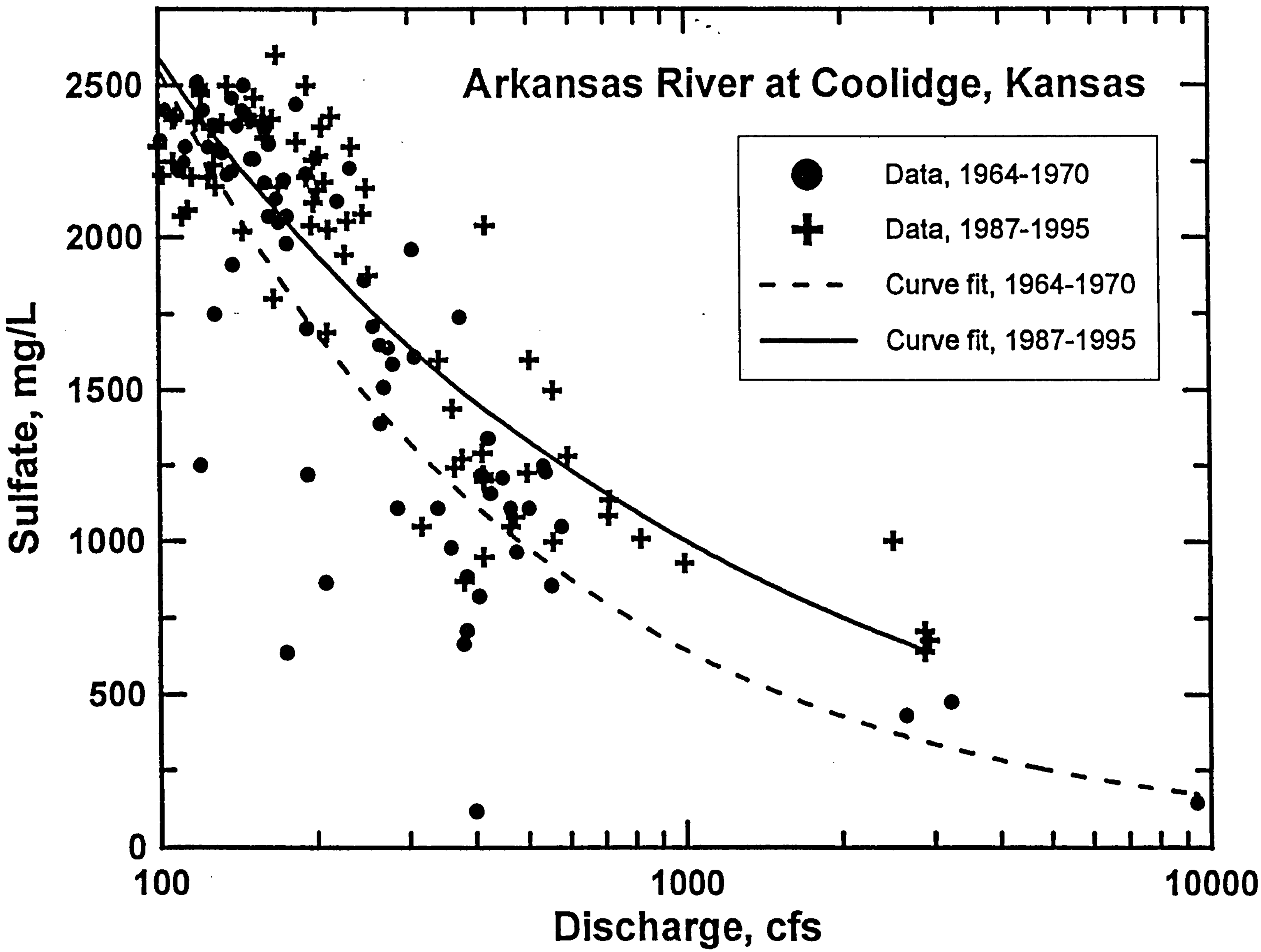

Figure 1.1 Relationship between sulfate concentration and discharge in the Arkansas River near Coolidge, Kansas.

groundwater has been mainly pumped from the deeper Ogallala aquifer in recent decades. Most wells in the region have been installed using reverse rotary drilling. Gravel packs are placed in the annular space between the well casing and the outer borehole surface through the screened interval. Gravel packs often extend upwards across the clay and silty clay layers as shown in Figure 1.2 (Whittemore and Butler, 1997). Except for public water supply wells and more recently drilled domestic wells, grout seals in the well annulus are either not present or extend only to 10 to 20 feet below the ground surface. The alluvial aquifer is usually between 20 and 50 feet thick. Thus, the saline water in the perched aquifer can easily enter the gravel pack flows down the gravel pack, and intrudes the Ogallala aquifer. The borehole skin has a permeability lower than the aquifer sediments because of the presence of the fine-grained drilling debris. The low-permeability skin initially extends along the entire borehole. However, most of the debris skin along the screened interval is removed after pumping started. Figure 1.2 is a schematic drawing showing before and after a well being used for water supply. As a result, the saline water in the upper aquifer can flow directly into the Ogallala aquifer through the screened interval. The other possible path for the saline water in the perched aquifer to reach the Ogallala aquifer is through the leaky clay layers. Quantitative evaluation of the saline water intrusion should be carried out.

It is probable that some areas with gravel-packed wells have salinity in the deeper portion of the Ogallala aquifer and lower concentrations in the upper portion depending on the location of the screened interval. This study focuses on the transport of saline water from the perched aquifer into the Ogallala aquifer due to these two mechanisms

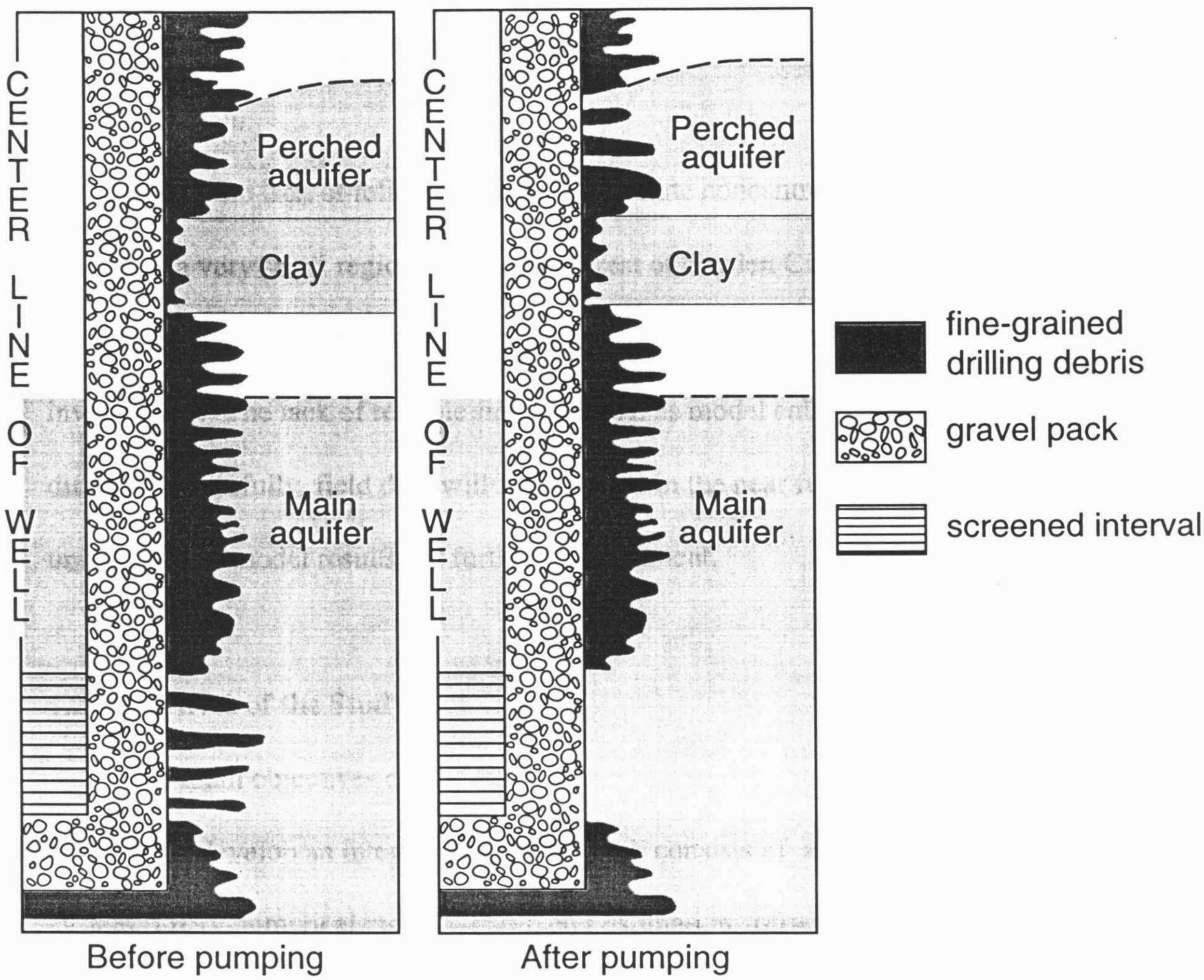

Figure 1.2 Before pumping and after pumping in a water supply well.

mentioned by using numerical models. A general purpose interactive system is developed to facilitate modeling effort in the GIS environment with a user interface. The user interface is customized within ARCVIEW as the command control to integrate ARC/INFO, numerical groundwater models, and a parameter-estimation software as a working system.

Due to the lack of reliable field data on solute concentration, the study area is limited to a very small region of Deerfield west of Garden City (Figure 1.3). Groundwater flow in the Garden City area not including solute transport is also investigated. The lack of reliable field data makes model calibration and validation very difficult. Hopefully, field data will be collected in the near future for evaluating the uncertainty of model results for further improvement.

1.2 Objectives of the Study

The main objectives of this study are:

1. To develop an integrated system which consists of a geographic information system (GIS), numerical models, parameter estimation software, and a graphical user interface such that modeling efforts can be carried out in interactive mode.

2. To estimate model parameters using available geological log data and universal kriging based on an inverse approach.

3. To apply the integrated system to estimate piezometric heads and solute concentrations in the High Plains aquifer near Deerfield under various conditions.

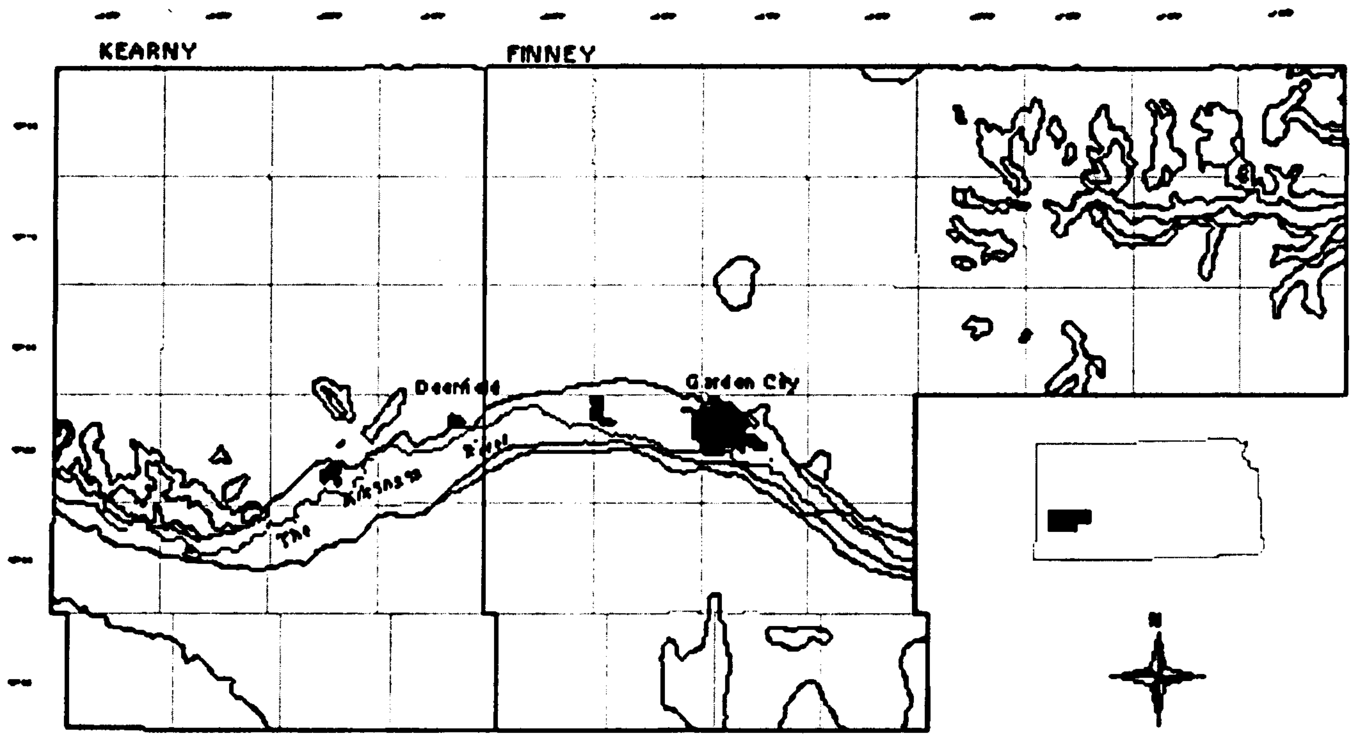

Figure 1.3 The location of the Deerfield area.

II. LITERATURE REVIEW

Mathematical groundwater models have become powerful tools to evaluate and manage groundwater resources in recent decades. Owing to increasingly serious groundwater contamination in recent years, much attention has been focused on the simulation of contaminant transport in the groundwater system. In a control theory approach, modeling dynamic systems comprises three fundamental steps: system characterization, system classification, and system identification. System identification includes model structure identification and parameter identification. The latter deals with parameter identifiability, parameterization, methods of parameter estimation, uncertainty about the estimated values of parameters, and uncertainty associated with prediction of the future behavior of the system (Yu, 1991). Groundwater flow and solute transport models relevant to this study are reviewed in this chapter. Some important publications on the application of GIS to water resources are also reviewed.

2.1 Groundwater Flow and Solute Transport Models

Solute-transport simulation is widely used to assess the alternative groundwater developments, the environmental impact and the design of groundwater contamination remediation programs.

Mangold and Tsang (1991) presented a review of 56 major numerical codes along with descriptions of the methods of analysis and their capabilities. These codes can be broadly classified as hydrologic transport models, geochemical models, and hydrochemial models.

If the velocity field of the groundwater flow is not affected by the solute concentration, then the velocity field can be calculated by using an existing groundwater flow model such as MODFLOW. The resulting velocity field can be used in the solute transport model such as MT3D for computing the solute concentration. However, the major uncertainty involves the parameter estimation, in particular, the dispersivities involved in the solute transport model. The U.S. Bureau of Reclamation (1993) investigated the water quality degradation of the Equus Beds aquifer in south-central Kansas through the conjunctive use of MODFLOW and MT3D. The objective was to determine how aquifer use affects the distribution of chloride. Ahlfeld and Zafirakou (1994) applied MODFLOW and MT3D to simulate groundwater flow and contaminant transport and combined with linear optimization technique to solve the groundwater contaminant remediation problem.

If the velocity field is affected by the solute concentration, a coupled approach must be taken. Ma (1996) studied the saltwater intrusion into the Great Bend aquifer in south-central Kansas by using the existing software SWIFT II (Reeves et al, 1986) which includes the effect of density gradient. The salt water intrusion in his study is due to the irrigation pumping which results in the upconing of deeper saltwater in the aquifer. The maximum chloride concentration of the saltwater is 28,000 mg/L and the corresponding density is 1036 kg/m^3. Therefore, the effect of density gradient on the velocity field must be included in modeling.

In this study, the usual maximum sulfate and total dissolved solids in highly contaminated concentrations portions of the aquifer are around 2300 mg/L and 4000 mg/L, respectively. The estimated density of the saline water based on data for sodium sulfate solutions is 1001.8 kg/m^3 at 20° C. The approximate density for fresh ground water with a dissolved solids concentration of 500 mg/L is 998.5 kg/m^3 at 20° C. The density difference between the saline and fresh groundwater is 3.3 kg/m^3 or about 0.3% of the density. In comparison with Ma's case, the density of the saline water in this study is not significant, thus the gravitational effect due to density gradient on the groundwater motion can be neglected. The velocity field computed using MODFLOW can be used in the solute transport model MT3D.

2.2 Parameter Identification and Parameterization

Groundwater flow and solute transport model parameters are continuous functions in space, hence the dimension of parameters can be infinite. Parameterization is a procedure to reduce the parameter dimension for use in numerical schemes. The methods for reducing parameter dimension can be classified as (Sun, 1994): (1) the zonation method, (2) the interpolation method, (3) the stochastic-field method, and (4) the geological structure method.

The zonation method is the most widely used in practical application. In this approach, the flow region may be divided into a number of homogeneous and isotropic zones. In each zone, the parameter(s) is constant. Optimal division of the zones is a difficult problem. Sun and Yeh (1985) noted that an incorrect zonation pattern can lead to large errors in estimated parameter values. One way to improve the zonation method is to estimate the parameter structure and parameter values to avoid both overparameterization and a priori zonation. Eppstein and Dougherty (1996) presented a method to simultaneously estimate transimissivities and zonation structure by combining an extended Kalman filter and an iterative partitional cluster algorithm.

Two common interpolation methods are found in groundwater literature. One is the finite-element interpolation method, and the other is the geostatistical interpolation method. It is extremely difficult to optimally determine the locations of nodes in the finite-element interpolation method. The geostatiscal interpolation method involves determining the unknown distributed parameter by employing kriging and pilot points (de Marsily et al, 1984; Keidser and Rosbjerg, 1991; LaVenue and Pickens, 1992). However, to obtain reliable kriging results, a relatively large sample size is needed that is not usually available for practical problems.

In the stochastic-field method, the unknown parameter is regarded as a random variable described by some statistical parameters such as the mean and covariance (Hoeksema and Kitanids, 1984; Dagan and Rubin, 1988; Sun and Yeh, 1992). However, the inverse solution hinges on the appropriate statistical assumptions and the structure of covariance functions. Justification of using such assumptions is a difficult task.

The common weakness of the first three methods is that the valuable geological structure information is not directly included in parameter estimation. Sun et al (1995) proposed the geological structure method which considers the local geological information in parameter estimation and is more reasonable for three-dimensional modeling. This method will be discussed in detail in Chapter IV and will be used in this study.

2.3 Model Parameter Estimation

The problem of aquifer parameter identification has been studied extensively during the last several decades. The inverse problem of parameter identification concerns the optimal determination of the parameters by using the observation of the dependent variable, such as peizometric head, of the governing equation. A paper by Yeh (1986) reviews the literature on this topic. Various techniques have been developed to solve the inverse problem of parameter identification. Neuman (1973) classified the techniques as the direct or indirect approach. The direct method uses the equation error criterion in formulating the inverse problem while the indirect method uses the output error criterion in the formulation. The equation error criterion requires substantially more field data for the dependent variable than for the output error criterion. Therefore, the indirect method has been mostly used in groundwater studies. The indirect method minimizes the function for the discrepancies between calculated and observed output by using mathematical optimization techniques. Publications using the indirect method for estimating groundwater flow parameters have appeared in various journals (Yeh, 1986). However, little published work exists for coupled flow and solute transport problems.

Strecker and Chu (1986) combined the method of characteristics (MOC) with quadratic programming to estimate both flow and transport parameters. In order to avoid numerical instability, they separated the estimation into two stages. In the first stage they estimated the transmissivity field using piezometric head data only, and in the second stage they estimated the dispersivity coefficients from measured solute concentration incorporating with the previously estimated transmissivity. The concentration data are a function of transmissivity, thus it is more reasonable to inverse transmissivities based on both head and concentration data in the first stage.

Wagner and Gorelick (1987) presented a weighted least-squares analysis for estimating flow and transport parameters simultaneously and also discussed parameter uncertainty for a hypothetical two-dimensional aquifer system.

Keidser and Rosbjerg (1991) extended the two-stage approach to a two-stage feedback procedure. The model parameters were divided into flow (transmissivities) and transport (dispersivities and initial concentration of sources) parameters. In the first stage they used both piezometric head and concentration to estimate transmissivities, given initial values of the source concentration and the dispersivities. In the second stage, they estimated the solute transport parameters by using estimated transmissivities in the first stage and the concentration data. By repeating the optimization of the first stage, they obtained the final estimates of transmissivities. They minimized the formulated objective function for both stages by using Levenberg-Marquardt's algorithm.

Wagner (1992) proposed a methodology which combined groundwater flow and solute transport simulation based on the maximum likelihood estimation without prior information. Xiang et al (1993) estimated coupled flow and solute transport parameters for steady flow. They proposed a weighted L_1 norm as the error measure between the vector of the observed heads and concentrations and the corresponding vector of the computed heads and concentrations. They applied sensitivity equation method to minimize the error. Their applications for two hypothetical groundwater problems included parameter estimation.

2.4 GIS-Modeling System

The input data of groundwater models vary with space and time. For a large groundwater system, a large amount of input data must be handled for numerical models. In addition, an iterative procedure is generally needed to assess the adequacy and accuracy of hydrogeological parameters and boundary conditions, thus visual comparison between simulated results and measurements is desirable for adjusting the parameters in each simulation. A geographic information system (GIS) provides an integrated platform to manage, analyze and display disparate data and can greatly facilitate the modeling effort in data compilation, model calibration, and display of model parameters and results. Furthermore, GIS can also be used to generate valuable information for decision-making through its ability to spatially overlay and process data.

Various applications of GIS in water resources have been published in the Proceedings of the Symposium on "Geographic Information Systems and Water Resources" (1993). DeVantier and Feldman (1993) reviewed several applications in hydrologic modeling including floodplain hydrology, erosion prediction/control, and water-quality prediction/control. Recently, the development of an integrated GIS with groundwater models has attracted the attention of many researchers. Watkins et al. (1996) described GIS applications in groundwater flow modeling and reviewed some existing programs which interface GIS and groundwater models. The simulation-GIS systems can be broadly classified into two types: (1) integrated GIS-groundwater models, and (2) groundwater models embedded in GIS.

The first approach uses a set of programs or an interface to transfer data between GIS and groundwater models. In other words, the data stored in a GIS database are transferred into input files of groundwater models and output data of the models are transferred back into GIS database after simulation. The disadvantage of this approach is that one set of data is stored twice, one in GIS database and the other in ASCII files. This approach requires minimum modification in GIS and groundwater models to avoid the errors in modifying GIS source code and/or groundwater models. Hence, it is widely adopted in many applications because of its simplicity. The enhanced way of this approach is to modify the groundwater models to directly read model inputs from GIS data files such as coverages in ARC/INFO instead of original ASCII files. Thus, only a GIS database is used and no data-transfer program is required. An example is MODFLOWARC (Orzal and McGrath 1992).

The work by Rifai et al. and El-Kadi et al., respectively, basically integrated GIS with some existing groundwater models through data transferring and a user interface. Rifai et al. (1993) integrated a GIS software SYSTEM 9 with a groundwater model WHPA (Blandford and Huyakorn, 1990) for delineating wellhead protection areas around public water-supply wells. They developed a graphical user interface (GUI) in C-language for user interaction. El-Kadi et al. (1994) integrated a GIS software MAPINFO with a two-dimensional flow and transport model known as MOC (Konikow and

Bredehoeft, 1978) and provided a customized graphical user interface by using MAPBASIC language included in MAPINFO.

The second approach is to embed the equations governing the groundwater flow and solute transport into GIS as intrinsic functions through modifying the GIS source code or writing macro programs to perform numerical calculations (Watkins et al., 1996). There is no data conversion in this approach. However, this approach requires a great deal of modification and it is a difficult task to incorporate complicated numerical procedures into GIS as intrinsic functions. As an example, McKinney and Tsai (1993) wrote macro programs to solve sets of finite-difference equations in a raster system. The different levels of discretization were applied in their study in order to minimize numerical errors and accelerate convergence. Tim et al (1996) embedded three simplified formulas into the ARC/INFO software to calculate three kinds of indices which indicate the susceptibility of groundwater to contamination by pesticides without involving any groundwater model simulation. They developed a GUI by using arc macro language (AML) included in ARC/INFO to facilitate the rapid appraisal of groundwater vulnerability.

In this study, the first approach is adopted because of its flexibility and simplicity. Two GIS softwares ARC/INFO and ARCVIEW are integrated with the groundwater models MODFLOW and MT3D and the parameter estimation software PEST. ARCVIEW is customized to serve as the user interface of the integrated system.

III. INTERACTIVE INTEGRATED MODELING SYSTEM

3.1 System Components

The main objective of developing an integrated modeling system is to provide a user-friendly system that integrates spatial database (ARC/INFO), groundwater models, and a parameter estimation software in the GIS environment, thereby permitting interactive model simulation and calibration through a graphical user interface. Figure 3.1 is a schematic diagram showing the four components. At the heart of the system are the groundwater models. These models draw on a variety of data from an ARC/INFO database. PEST is parameter estimation software which facilitates the model calibration effort. Interactions with the user and presentation of information are through ARCVIEW customized by using AVENUE codes. These elements are described in more details below. An application of the integrated system is presented in Chapter V.

3.2 ARC/INFO

A geographic information system (ARC/INFO) stores spatial data which are required as input to execute numerical models. A ground surface contour coverage can be generated through triangulated irregular network (TIN), a type of surface modeling in ARC/INFO, or digitizing based on some point measurements and USGS topographic maps. The data of soil types and irrigation fields, which are related to recharge in the groundwater model, are stored in the polygon coverages. The rainfall data, streamflow data, well logs, pumpage, and groundwater levels are stored in the point coverages. The

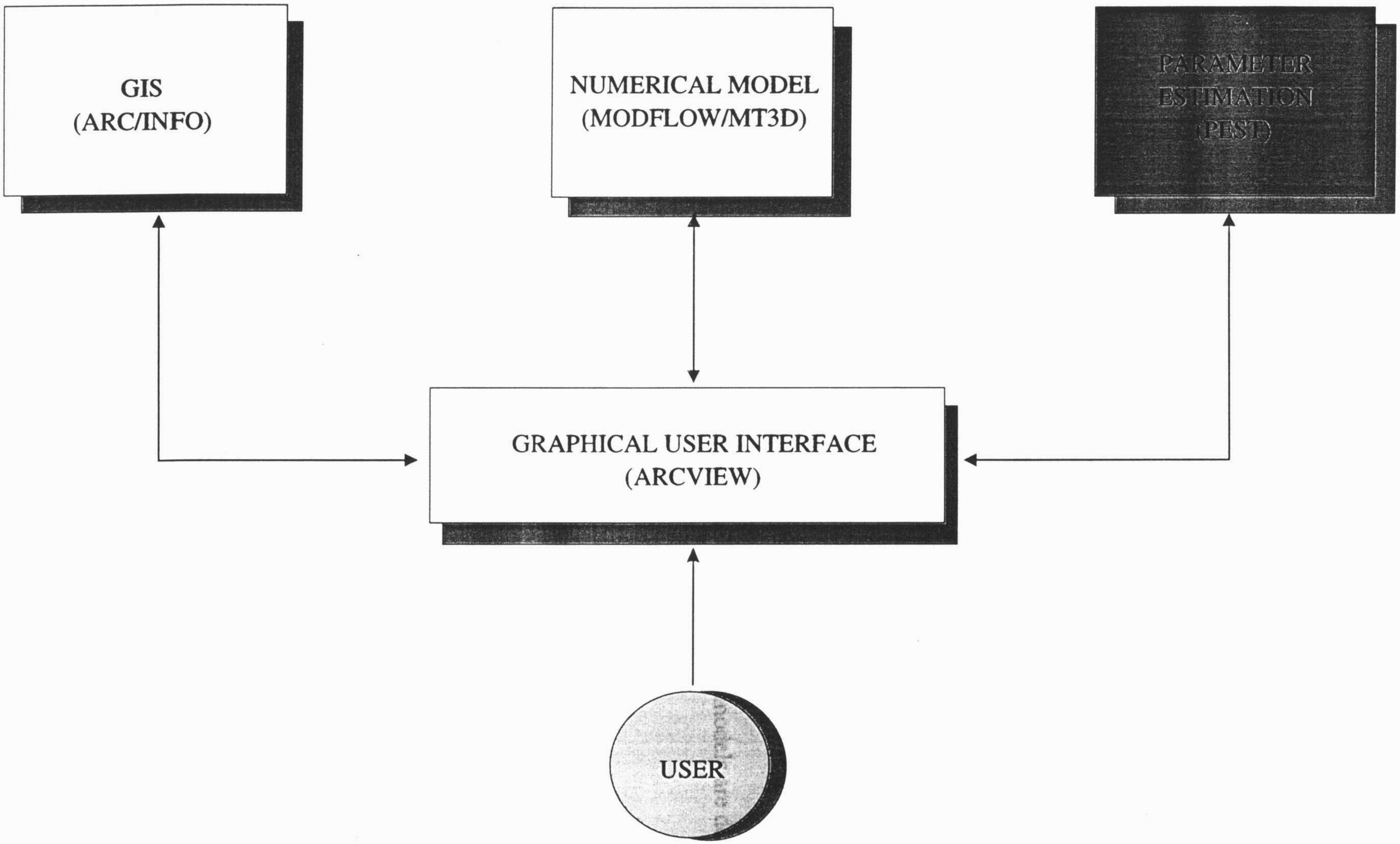

Figure 3.1 Components of the integrated system

data related to the Arkansas River and irrigation canals are stored in the line coverages. Also, the hydrogeological information such as hydraulic conductivity can be stored as coverages. These data can be transferred into groundwater models through the user interface in ARCVIEW.

3.3 Software for Numerical Models and Parameter Estimation

The widely used, three-dimensional finite-difference, groundwater flow model MODFLOW (McDonald and Harbaugh, 1988) is used in this study to simulate the flow field of the study area. The velocity components computed from MODFLOW are incorporated into the solute transport model MT3D (Zheng, 1992) to simulate the movement of the saline water. The computation and display of model outputs are controlled by the user in interactive mode on ARCVIEW. These models are described in more detail in the next chapter.

The parameter estimation software PEST (model-independent parameter estimation) (Doherty, 1994) is based on the weighted least squares method using the Lvenberg-Marquardt algorithm to solve the inverse problem for parameter estimation. This approach is described in more detail in the next chapter. In addition, the contours of optimized model outputs can be automatically shown on the screen after the execution of PEST.

3.4 Graphical User Interface ARCVIEW

The graphical user interface (GUI) of the integrated system is customized within ARCVIEW as the main command control that provides the access to various components of the system and performs the customized functions under the user's command. It is used not only for displaying the data stored in the database but also for estimating model parameters and executing simulations. The user customized functions are displayed as tool bars or button bars on the ARCVIEW screen.

ARCVIEW (ESRI, 1994) is a desktop GIS, which facilitates the organization, display, querying, analysis and publication of data. There are six specific terms used in ARCVIEW: PROJECT, VIEW, TABLE, CHART, LAYOUT, and SCRIPT. PROJECT is an ASCII file composed of VIEW, TABLE, CHART, LAYOUT and SCRIPT (Figure 3.2). VIEW is the main element in ARCVIEW and is an interactive map which allows users to display, explore, query, and analyze geographic data. Actually, it is a collection of geographic features, called themes, which can be an ARC/INFO coverage, an ARCVIEW shapefile, a simple format for storing the locations and attributes of geographic features, or an image data source. TABLE stores attributes of spatial data. The user can add dBASE, INFO or text files to ARCVIEW as tables or can connect to a database server, such as ORACLE, to retrieve records as tables. CHART is a graph of tabular data which provides an additional representation of the attributes of geographic features. LAYOUT generates a map from ARCVIEW. SCRIPT contains AVENUE code to expand the capabilities of ARCVIEW to applications desired by the user.

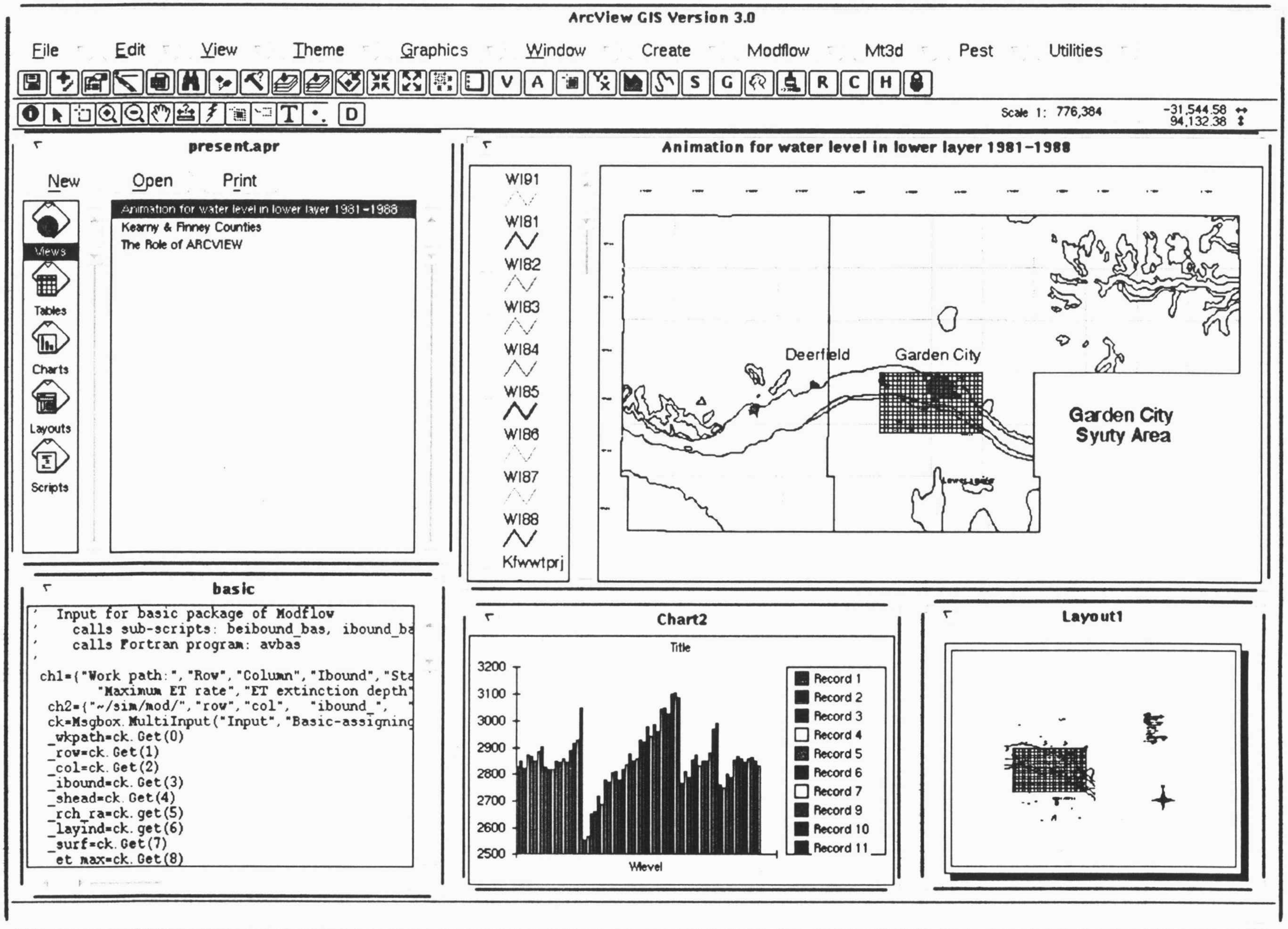

Figure 3.2 Components of an ARCVIEW PROJECT.

ARCVIEW has several advantages over other commercial software as the user interface: (1) its graphic user interface is user-friendly, (2) its flexibility in linking external softwares is a desired feature for use as the common platform for an integrated system, (3) it can communicate with ARC/INFO. In this study, ARCVIEW serves as a client and ARC/INFO as a server. ARCVIEW can send requests to ARC/INFO to execute some spatial operation structured by using Arc Macro Language (AML) through the software interapplication communication (IAC). The client and server can be placed on different machines of a network, (4) ARCVIEW shares the same tables of attributes with INFO in an input coverage.

Figure 3.2 shows the customized user interface composed of a menu bar, a button bar and a tool bar within the ARCVIEW environment. Five menus, “Create”, “Modflow”, “Mt3d”, "Pest" and “Utilities” are added in the user interface. Some frequently used functions listed on the menus are also customized as buttons on the second row of the interface. The description of a button or selected menu item is listed in the status bar at the bottom of the screen.

3.5 Modeling Implementation

The procedure of modeling implementation consists of model-grid generation, input data preparation, model calibration, simulation, and display of results in the GIS environment. They are described in the following sections.

3.5.1 Model-Grid Generation

Grids of the numerical model are generated as a polygon coverage in the vector-based GIS whereas points located at the center of a grid cell are represented as a point coverage, called a grid-point coverage in this study. Model parameters are stored at each point. The advantage of a vector-based model for generating grids is that the grid cell sizes can be readily varied by changing the polygons. Grids over the modeling area of interest are generated as a shapefile in two ways. One is to specify the coordinates of the lower left point and upper right point and cell size, while the other is to create a rectangular region and specify column and row numbers. The grids can also be rotated. Since the groundwater flow model is based on the assumption that the Cartesian coordinates x, y and z are the principle directions of the hydraulic conductivity tensor, it is necessary to rotate the grids to be parallel to the groundwater flow direction.

3.5.2 Input Data Preparation

Hydrogeologic input data for groundwater models are stored in the coverages of ARC/INFO. They can be transferred to the grid-point coverage by interpolation using TIN (triangular irregular network) in ARC/INFO. Also, users can edit the attributes of the grid-point coverage in graphical form in VIEW or in tabular form in TABLE.

Since both MODFLOW and MT3D have a modular structure with different model packages, each package needs different input data files in different formats. Therefore, the data in the grid-point coverage must be exported from INFO in the required input format to the groundwater model packages through relational query and calling external FORTRAN codes in the user interface ARCVIEW.

3.5.3 Model Calibration, Simulation, and Display of Results

MODFLOW and MT3D are executed through the user interface. The computed results such as piezometric head or solute concentration can be compared with the measured values in a display by overlaying two respective data layers. Also, the difference between computed and measured values can be displayed as residual contours for identifying areas of large discrepancies for further modification.

The final simulated results can be shown as line drawings or in colored grid cells with different overlaying layers of coverages such as city locations, land uses and so on in VIEW. Also, it is convenient to generate a map from LAYOUT by bringing in the VIEW, adding descriptions in the layout, and sending the layout to a printer or a plotter. The selected themes in VIEW can be shown continuously as a film through animation. For example, water level in different years can be selected and shown continuously to observe the changes.

IV. GROUNDWATER FLOW AND SOLUTE TRANSPORT MODELS

4.1 Groundwater Flow Model

MODFLOW is a widely used program developed by McDonald and Harbaugh (1988) for solving unsteady, three-dimensional groundwater flow problems using the finite-difference scheme. This is a physical law based model. The governing equation for the dependent variable h (piezometric head) derived from Darcy's law and the continuity equation can be written as (see, for example, Rushton and Redshaw, 1979):

$$\frac{\partial}{\partial x}\left(K_x \frac{\partial h}{\partial x}\right)+\frac{\partial}{\partial y}\left(K_y \frac{\partial h}{\partial y}\right)+\frac{\partial}{\partial z}\left(K_z \frac{\partial h}{\partial z}\right)-W=S_s \frac{\partial h}{\partial t} \qquad (4.1)$$

where

K_x, K_y, K_z = hydraulic conductivities in the principle axes directions of x, y and z, respectively (LT^{-1}),

h = the piezometric head at (x, y, z, t) (L),

W = the volume flow rate per unit volume for a source (positive) or a sink (negative) (T^{-1}),

S_s = the specific storage of the porous material defined as the volume of water released from storage per unit change in piezometric head per unit volume of aquifer material (L^{-1}),

t = the time (T).

The velocity components in Eq. 4.1 are given by Darcy's law

$$v_x = -K_x \frac{\partial h}{\partial x}\ ,\ v_y = -K_y \frac{\partial h}{\partial y}\ ,\ v_z = -K_z \frac{\partial h}{\partial z} \tag{4.2}$$

In general, S_s, K_x, K_y, and K_z are functions of x, y, and z and W is a function of x, y, z, and t. Eq. 4.1 describes the movement of groundwater with constant density in a heterogeneous and anisotropic medium, provided that x, y, and z are the principal axes of the hydraulic conductivity tensor.

Eq. 4.1 together with specified boundary and initial conditions forms the mathematical model for groundwater flow. MODFLOW uses the block-centered finite-difference method to solve numerically Eq. 4.1. An example of spatial discretization is shown in Figure 4.1.

4.2 Solute Transport Model

The equation governing the unsteady, three-dimensional, solute transport in groundwater without chemical reactions can be written as follows (Zheng, 1992):

$$\frac{\partial C}{\partial t} = \frac{\partial}{\partial x}\left(D_x \frac{\partial C}{\partial x}\right) + \frac{\partial}{\partial y}\left(D_y \frac{\partial C}{\partial y}\right) + \frac{\partial}{\partial z}\left(D_z \frac{\partial C}{\partial z}\right)$$

$$-\left[\frac{\partial}{\partial x}(u_x C) + \frac{\partial}{\partial y}(u_y C) + \frac{\partial}{\partial z}(u_z C)\right] + \frac{W}{\theta} C_s \tag{4.3}$$

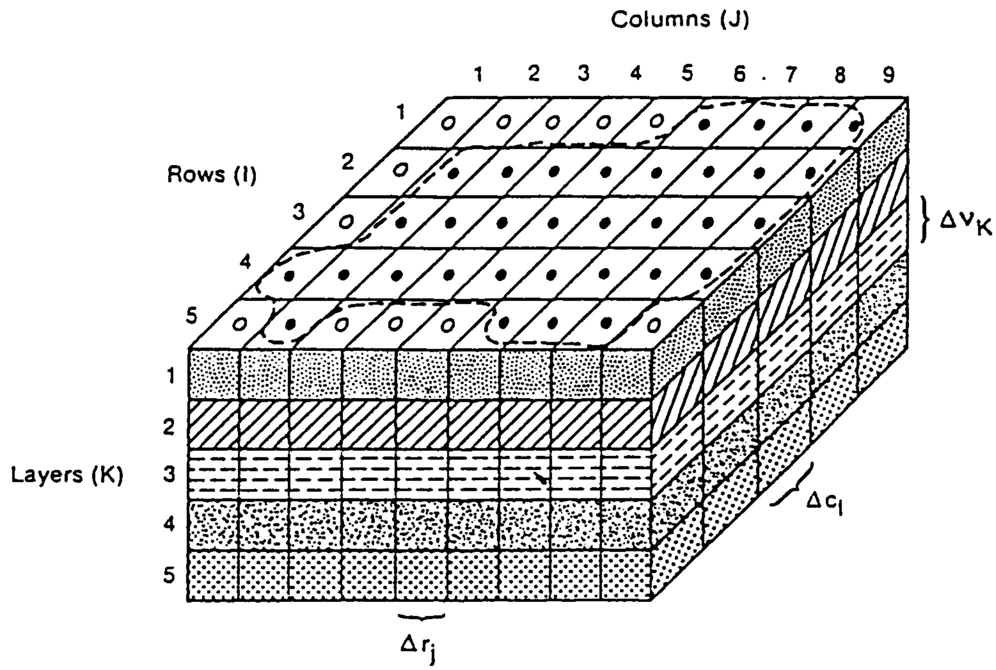

Explanation

- - - - Aquifer Boundary

• Active Cell

o Inactive Cell

Δr_J Dimension of Cell Along the Row Direction. Subscript (J) Indicates the Number of the Column

Δc_I Dimension of Cell Along the Column Direction. Subscript (I) Indicates the Number of the Row

Δv_K Dimension of the Cell Along the Vertical Direction. Subscript (K) Indicates the Number of the Layer

Figure 4.1 Spatial discretization of an aquifer system (after McDonald and Harbaugh, 1988).

where

C = the solute concentration in groundwater (ML^{-3}),

t = the time (T),

D_x, D_y, D_z = the hydrodynamic dispersion coefficients in the direction of the principal axes x, y, z, respectively (L^2T^{-1}),

θ = the porosity of porous medium,

u_x, u_y, u_z = the seepage velocity components in x, y, z directions, respectively, and equal to the Darcy velocity in Eq. 4.1 divided by the porosity (LT^{-1}),

W = the volume flow rate of water per unit volume of aquifer from a source (positive) or a sink (negative) (T^{-1}),

C_s = the concentration of the source or sink (ML^{-3}).

The three terms on the right side of Eq. 4.3 are from left to right: the dispersion term, the advection term, and the sink or source term. Equation 4.3 can also be written as

$$\frac{DC}{Dt}=\frac{\partial}{\partial x}\left(D_x\frac{\partial C}{\partial x}\right)+\frac{\partial}{\partial y}\left(D_y\frac{\partial C}{\partial y}\right)+\frac{\partial}{\partial z}\left(D_z\frac{\partial C}{\partial z}\right)-\frac{W}{\theta}(C-C_s) \qquad (4.4)$$

where $\frac{DC}{Dt} = \frac{\partial C}{\partial t} + u_x \frac{\partial C}{\partial x} + u_y \frac{\partial C}{\partial y} + u_z \frac{\partial C}{\partial z}$, indicates that the time rate of change is calculated along the pathline of a contaminant particle (or a characteristic curve of the velocity field). By introducing the finite difference algorithm, the substantial derivative in an Eulerian grid system becomes

$$\frac{DC}{Dt} = \frac{C_m^{n+1} - C_m^{n^*}}{\Delta t} \tag{4.5}$$

so that Eq. 4.4 becomes

$$C_m^{n+1} = C_m^{n^*} + \Delta t \times [\text{RHS of Eq. 4.4}] \tag{4.6}$$

where

C_m^{n+1} = the average solute concentration for cell m at the new time level (n+1),

$C_m^{n^*}$ = the average solute concentration for cell m at the new time level (n+1) due to advection alone, also refer to as the intermediate time level (n^*)

Δt = the time increment,

Equation 4.6 constitutes the basic algorithm of the mixed Eulerian-Largrangian method by solving the advection term with a Largrangian method and the dispersion term with an Eulerian method. In MT3D, the Largrangian approach employs the method of characteristics by using the particle tracking technique and the Eulerian approach utilizes the block-entered finite-difference method.

4.3 Parameterization and Model Parameter Estimation

In the study area of Deerfield, drillers' well logs have been filed since 1975. There are 36 drillers' logs available over an area of 57.1 km^2, which is larger than the minimum required sample number of 30 for accurate kriging estimation. For lack of any field test data on the hydraulic conductivity, the lithologic data in the well log are used as the basis for estimating the hydraulic conductivity. The lithologic logs are analyzed to characterize the composition of geological materials and the thickness of each material for each log. The thickness of the each geological layer in the study area is estimated by universal kriging based on the data derived from the 36 well logs. For each geological material, the upper and lower bounds of the hydraulic conductivities are determined based on published values. The hydraulic conductivity for each block in the numerical scheme is taken as the thickness-weighted value. The optimal values of the hydraulic conductivity of geological materials are estimated by solving the inverse problem. These estimated values can then be used in the study. The following sections describe universal kriging and parameter estimation.

4.3.1 Estimating Layer Thickness Using Universal Kriging

A sample lithologic log is shown in Figure 4.2, in which different geological materials and thicknesses below the ground surface at the well location are identified.

Figure 4.2. A sample lithologic log. The actual record has more divisions of materials; these have been summarized into fewer divisions below. The arrows refer to clay zones separating higher permeability layers of the aquifer system.

City of Deerfield Public Water Supply Well Drilled 1978

Depth, ft		Thickness, ft		Description of sediment
0 -	9	9		Top soil
9 -	47	38	⇔	Brown clay
47 -	74	27		Fine - medium sand & gravel
74 -	96	22	⇔	Brown clay
96 -	108	12		Fine - medium sand
108 -	226	118	⇔	Brown & blue clays, 2 sand streaks
226 -	230	4		Fine - medium sand, fine gravel
230 -	239	9	⇔	Brown clay, small sand streak
239 -	253	14		Fine - medium sand & gravel
253 -	274	21		Fine - medium sand & gravel, 10% clay
274 -	303	29	⇔	Brown clay
303 -	338	35		Fine - medium sand & gravel, 10% clay
338 -	351	13	⇔	Brown sandy clay, sticky
351 -	365	14		Fine sand, 10% clay
365 -	393	28		Fine - medium sand & gravel, gravel streak (Screened interval 364 - 394 ft)
393 -	397	4	⇔	Brown clay (Bottom of well at 397 ft)

The thickness of the ith geological material is designated as b_i for $i = 1, 2, \dots, L$. L is the number of geological layers within an aquifer.

An aquifer system is discretized into a number of rectangular blocks with the center of a block representing the grid node (Figure 4.1). Each block may contain several different geological materials with varying thickness. From the 36 well logs, universal kriging is employed to estimate the thickness at locations where no well-log data are available.

Let $b_i(x,y)$ represent the thickness of the i th geological layer at an unsampled site. The thickness $b_i(x,y)$ is a nonstationary spatial random function with a trend given as

$$b_i(x,y) = m_i(x,y) + r_i(x,y) \tag{4.7}$$

where

$m_i(x,y) = E\{b_i(x,y)\}$, the trend,

$r_i(x,y)$ = the deviation from the trend.

Universal kriging involves three steps: (1) the trend $m_i(x,y)$ must be estimated and removed, (2) the stationary residual $r_i(x,y)$ is kriged to obtain the needed estimates, (3) the estimated residual is combined with the trend to obtain the estimate of thickness $b_i(x,y)$. The computation of universal kriging can be performed using the software KTB3D in GSLIB (Deutsch and Journel, 1992).

4.3.2 Block Parameter Estimation

After the thickness distribution for each geological layer is estimated by universal kriging, the thickness-weighted hydraulic conductivity and storativity of a rectangular block can be estimated. In this study, the horizontal hydraulic conductivities in x and y directions are assumed to be equal ($K_H = K_x = K_y$) and the vertical hydraulic conductivity $K_V = K_z$. The thickness-weighted distributed parameters K_H, K_V, and S can be obtained for each block (Figure 4.3) by the following equations:

$$K_H(x_{ijk}) = \sum_{n=1}^{N_{ijk}} b_{ijk}^n K_{ijk}^n / b_{ijk} \tag{4.8}$$

$$K_V(x_{ijk}) = b_{ijk} / \sum_{n=1}^{N_{ijk}} \left(b_{ijk}^n / K_{ijk}^n \right) \tag{4.9}$$

$$S(x_{ijk}) = \sum_{n=1}^{N_{ijk}} b_{ijk}^n S_{ijk}^n / b_{ijk} \tag{4.10}$$

where

x_{ijk} = the identification of a block in which i, j, and k indicate the number of the row, the column, and the model layer, respectively,

N_{ijk} = the number of geological layers in the block,

b_{ijk}^n = the thickness of the nth layer in the block, where n = 1, 2, ... , N_{ijk},

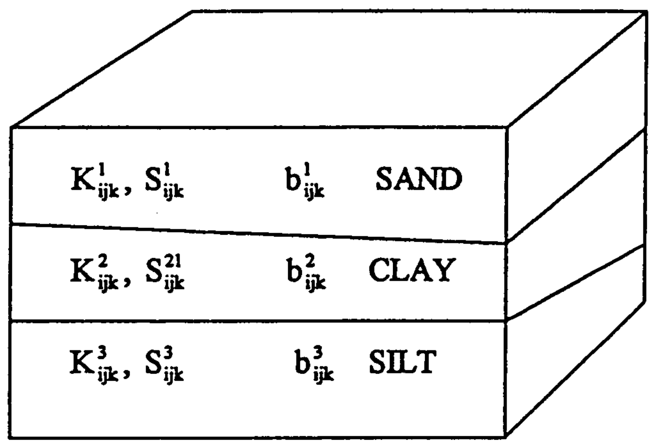

Figure 4.3 An example for three geological materials in a block (ijk).

$$b_{ijk} = \sum_{n=1}^{N_{ijk}} b_{ijk}^{n} ,$$

K_{ijk}^{n} = the hydraulic conductivity associated with the nth geological material,

S_{ijk}^{n} = the storativity associated with the nth geological material.

By using Eqs. 4.8, 4.9, and 4.10, distributed parameters K_H, K_V, and S for each block can be estimated from the solution of the inverse problem.

4.3.3 Estimation of Optimal Parameters

If the field measurements of solute concentration are also available, then the simultaneous estimation of groundwater flow and solute transport parameters can be conducted by minimizing the weighted sum of squared errors between calculated and observed piezometric head and solute concentration data. In this study, because of scarcity of solute concentration data, the estimation of dispersion parameters would be unreliable. Thus, only the estimation of the groundwater flow parameters will be conducted.

Let u^{obs} be a vector of the observed piezometric heads and u(p) a vector of computed piezometric heads with parameter vector p. The vector e is the difference of the observed and computed piezometric heads.

$$e = u^{obs} - u(p) \tag{4.11}$$

The optimal estimates of model parameters minimize the following weighted squares of errors:

$$Z = e^T we = \left(u^{obs} - u(p)\right)^T w\left(u^{obs} - u(p)\right) \tag{4.12}$$

where

T = transpose,

w = a diagonal weighting matrix indicating the reliability of u^{obs}.

The values of the hydraulic conductivity and the storativity of geological materials have upper and lower bound as given in textbooks (See, for example, Freeze and Cherry, 1979). For instance,

$$10^{-2} < K_{sand} < 10^{-5} \text{ (m/sec)} \tag{4.13}$$

$$10^{-9} < K_{clay} < 10^{-12} \text{ (m/sec)} \tag{4.14}$$

The objective function, Eq. (4.12), subject to constraints such as Eqs. 4.13 and 4.14 forms a nonlinear optimization problem. It can be solved in PEST (Doherty, 1994) by combining with groundwater models. In order to obtain reasonable estimates of parameters, the number of parameters must be less than the number of observations. The distributed values of hydraulic conductivity and storativity over the entire aquifer under study can be obtained from Eqs. 4.8, 4.9, and 4.10 using the estimated parameter vector from the solution of the inverse problem.

V. RESULTS AND DISCUSSION

The integrated system is applied to evaluate the groundwater system near Garden City, Kansas. The zonation method instead of the geological structure method was used in parameter estimation. Because solute concentration data of sufficient detail are not available in the area, only the groundwater flow simulation was conducted. The solute transport will be included in the study of a small region of Deerfield. To investigate the effect of the saline water moving into the fresh groundwater, a conceptual model is proposed and the solute transport is modeled numerically in a hypothetical aquifer. The results are presented here.

5.1 An Application of The Integrated System

The integrated system was applied to the Garden City area in southwestern Kansas (Figure 3.2) to evaluate the groundwater flow. The pre-development groundwater condition prior to the 1950s is simulated. The flow is assumed to be steady (Dunlap, 1985). The High Plains aquifer within the Arkansas River valley comprises two layers: the alluvial aquifer and the underlying Ogallala aquifer separated by a layer of discontinuous clay within the valley. Elsewhere the High Plains aquifer is treated as one unit.

Sources of recharge to the aquifer system are infiltration from precipitation and irrigation water, seepage from the Arkansas River and irrigation canals, and subsurface inflow at the boundaries of the study area. Recharge from precipitation during the growing season (April-October) is assumed to be 10 percent of mean annual precipitation of 45.67 cm on irrigated land and 1 percent of the precipitation on nonirrigated land (Gutentag and Stullken, 1976). The exact contribution of infiltration from irrigated fields and canals to the aquifer could not be calculated due to the absence of field data. Approximately 25 percent of the applied irrigation water was estimated to infiltrate into the aquifer (Meyer et al, 1970).

Figure 5.1 shows a grid composed of 14 rows and 24 columns covering the study area. The spatial attributes of each cell are stored at the center of each cell. The initial water level was based on the observations of the year 1940, and the values at unobserved cells were interpolated using TIN described in Section 3.5.2. In the upper layer, the northern and southern boundaries along the boundary of the alluvial valley are set as the no-flow condition since groundwater mainly exists in the lower Ogallala aquifer outside the alluvial valley, and the piezometric head boundaries are set at the eastern and western boundaries. In the lower layer, the piezometric head boundaries are set around the area. After generating all descriptive data, GIS functions can be used to list or display the hydrological data for inspection.

In this application, the optimal hydraulic conductivity of each zone in both layers is estimated by employing PEST. The observed and computed contours of piezometric head in the lower layer are shown in Fig. 5.1. Also, the differences between the observed and computed values are shown in Figure 5.1. The results show that reasonable agreement is obtained.

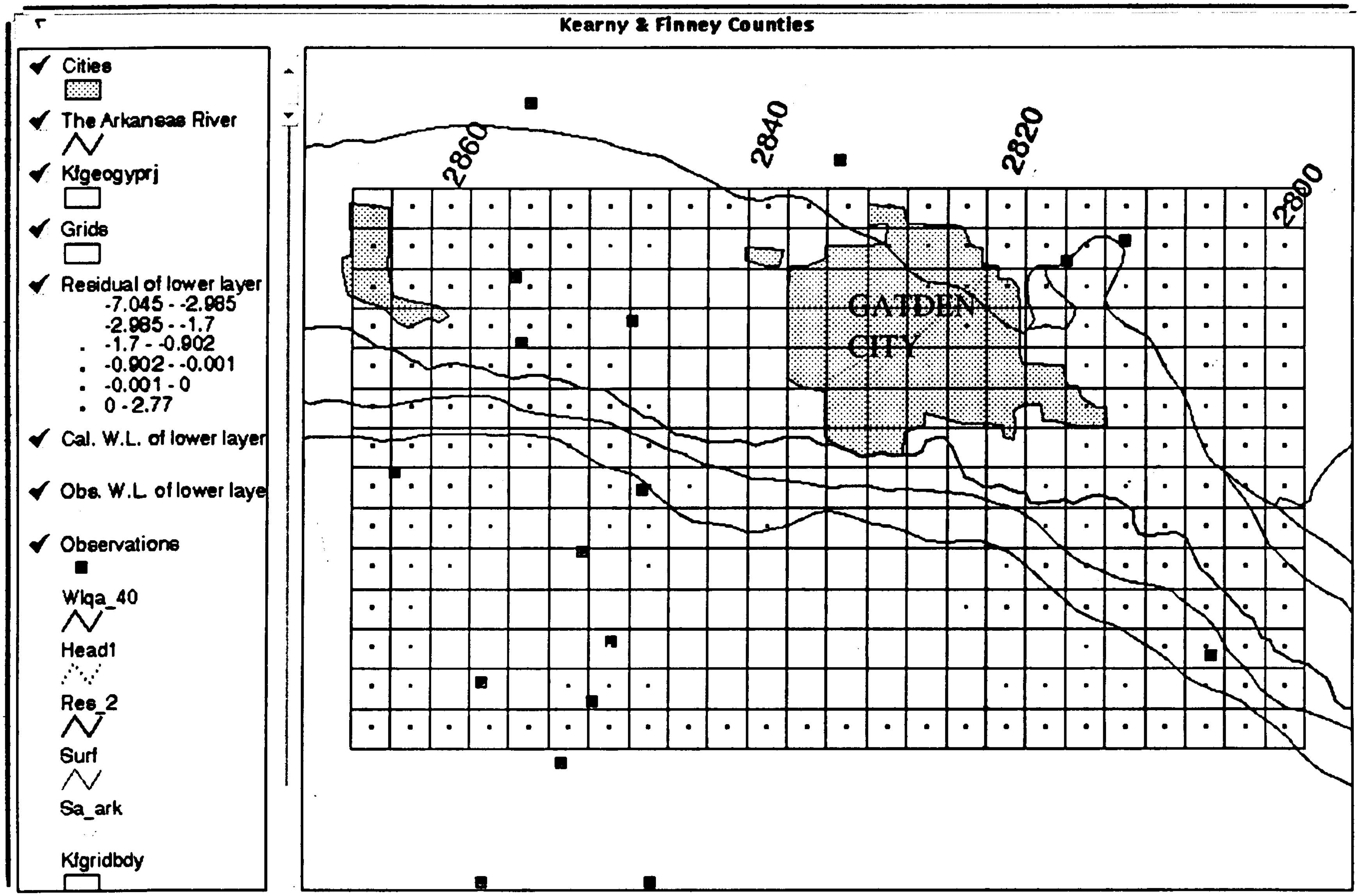

Figure 5.1 Contours of observed and conputed piezometric head and residual ranges for the lower layer.

5.2 A Conceptual Model for Saline Water Intrusion

A conceptual model is proposed based on the observation that the saline water in the upper aquifer can flow through the gravel pack of a well down into the lower Ogallala aquifer. This conceptual model is simulated numerically to estimate the spreading of the saline water in the freshwater aquifer. Areal recharge and evapotranspiration are not involved. The leakage of the saline water through the clay layer will be included later. The constant head boundaries are set in the western and eastern boundaries as 859 m and 857 m above the mean sea level, respectively. The north and south boundaries of the study area are no-flow boundaries. The initial water table is assumed to decrease linearly from the west to the east based on the specified boundaries. The background sulfate concentration is 30 mg/L. The steady downward flow rate of the saline water through the gravel pack in the irrigation well is estimated to be 200 m^3 / day (~ 36 gpm) based on the Thiem equation (Fetter, 1994). The sulfate concentration of the saline water in the upper aquifer is 2000 mg/L. Based on the conceptual model, simulations for a single well and multiple wells are carried out and described as follows.

5.2.1 A Single Well Source

A hypothetical aquifer with an area of 1200 m by 400 m and a depth of 80 m is used for the simulation. The point source of saline water from an irrigation well is located at the center of the area. The model grid has 27 rows, and 43 columns as shown in Fig. 5.2, and 8 layers. In the X and Y directions, variable spacings ranging from a minimum of 5 m to a maximum of 50 m are used to meet the accuracy requirement. The aquifer is

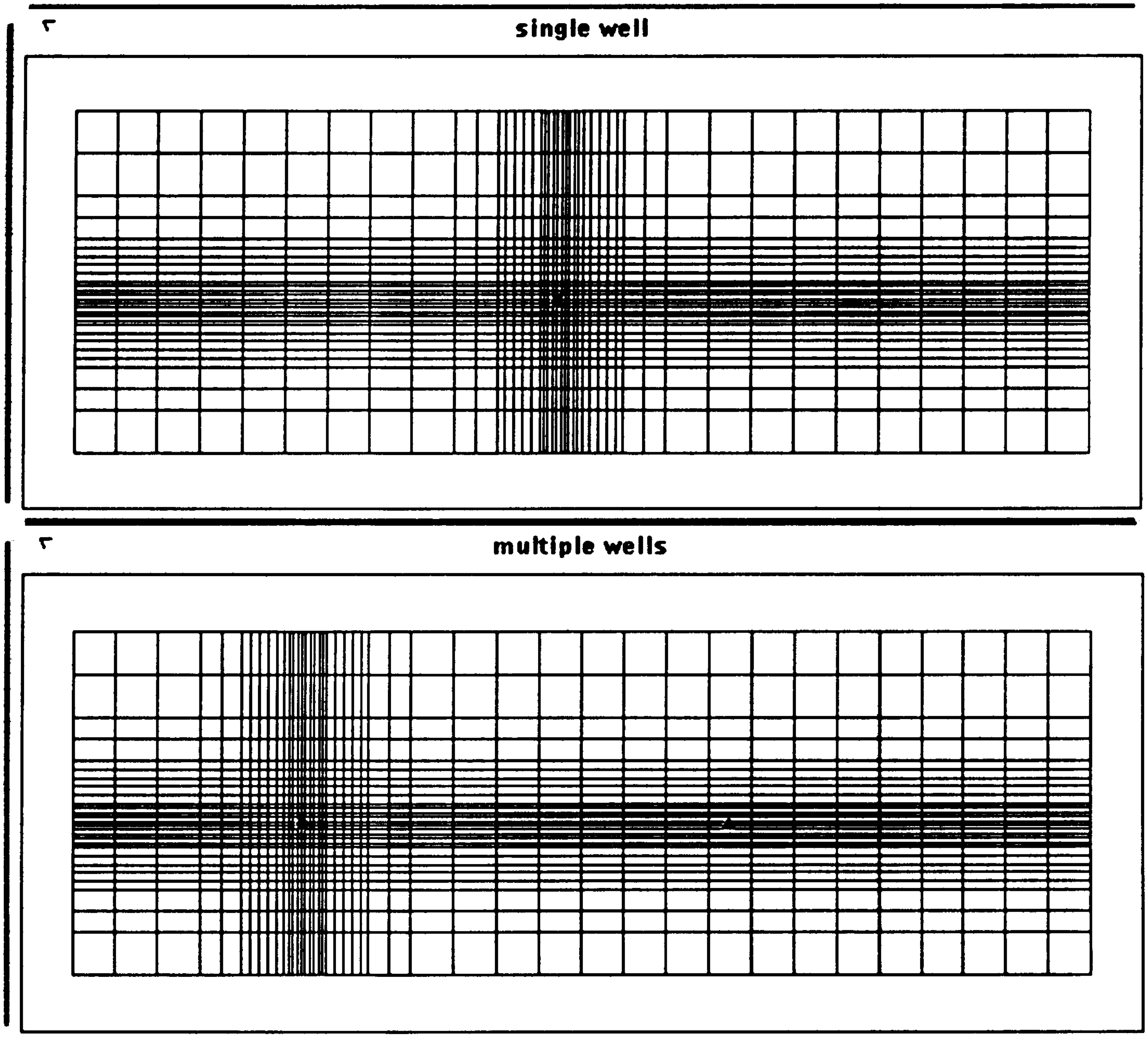

Figure 5.2 Model grids for single well and multiple well cases. The red dot is the irrigation well. The green triangle is the municipal well.

divided into eight 10-m layers. Finer grid sizes and smaller layer thickness are also investigated.

Four cases are considered and described in Table 5.1. The values of variables and parameters used in these cases are summarized in Table 5.2. These values are commonly used in the literature (Bureau of Reclamation, 1993). The irrigation well generally pumps water from the deeper portion of the aquifer through a 30-meter well screen extended from a depth interval of 50 to 80 meters (layers 6-8) below the confining layer in the conceptual model. Because of the existence of a lower permeability skin around the borehole, most of the saline water probably enters the aquifer through the upper part of the well screen during extended periods when the well is not pumped. A major portion of the saline water enters the sixth layer and the rest is distributed to layers 1-5. Cases 1 and 2 are without pumping. In Case 1, the inflow rate in layer 6 is 75% of $200\ m^3/day$ and the rate for each of the layers 1 to 5 is 5% of $200\ m^3/day$. In Case 2, the inflow rate in layer 6 is 50% of $200\ m^3/day$ and the rate for each of the layers 1 to 5 is 10% of $200\ m^3/day$. Cases 3 and 4 include pumping of the irrigation well at a rate of $4360\ m^3/day$ (~ 800 gpm). The well is pumped in May, July, and August. In the pumping cases, part of the saline water that had entered the aquifer during periods of no pumping is removed, as well as the concurrent flow down the gravel pack.

Representative results for Case 3 are shown in Fig. 5.3. The hydraulic gradient is 0.0017 and the hydraulic conductivity is 10 m/day, so the uniform velocity for the area without source or sink is 0.017 m/day. The inflow rate in layer 3 is 10 m^3/day and the rate is distributed to six faces of the cell where the well is located. The eastward and

Table 5.1 Cases for single well simulation.

Case	Location of point source	Source strength	Total flowrate of saline water	Pumping
1	Layers 1-5 Layer 6	10 m^3/day each 150 m^3/day	200 m^3/day	no
2	Layers 1-5 Layer 6	20 m^3/day each 100 m^3/day	200 m^3/day	no
3	Layers 1-5 Layer 6	10 m^3/day each 150 m^3/day	200 m^3/day	4360 m^3/day in May., Jul., and Aug.
4	Layers 1-5 Layer 6	20 m^3/day each 100 m^3/day	200 m^3/day	4360 m^3/day in May., Jul., and Aug.

Table 5.2 Values of variables and parameters used in the numerical simulation

Aquifer and other parameters	
horizontal hydraulic conductivity	K_h = 10 m/day
vertical hydraulic conductivity	K_v = 0.001 m/day
specific yield	S = 0.2
porosity	θ = 0.5
longitudinal dispersivity	α_L = 30 m
lateral dispersivity	α_{HT} = 9 m
vertical dispersivity	α_{VT} = 9 m
depth to bedrock	80 m
irrigation pumpage	4360 m^3 / day
initial sulfate concentration	30 ppm
total simulation time	1 year

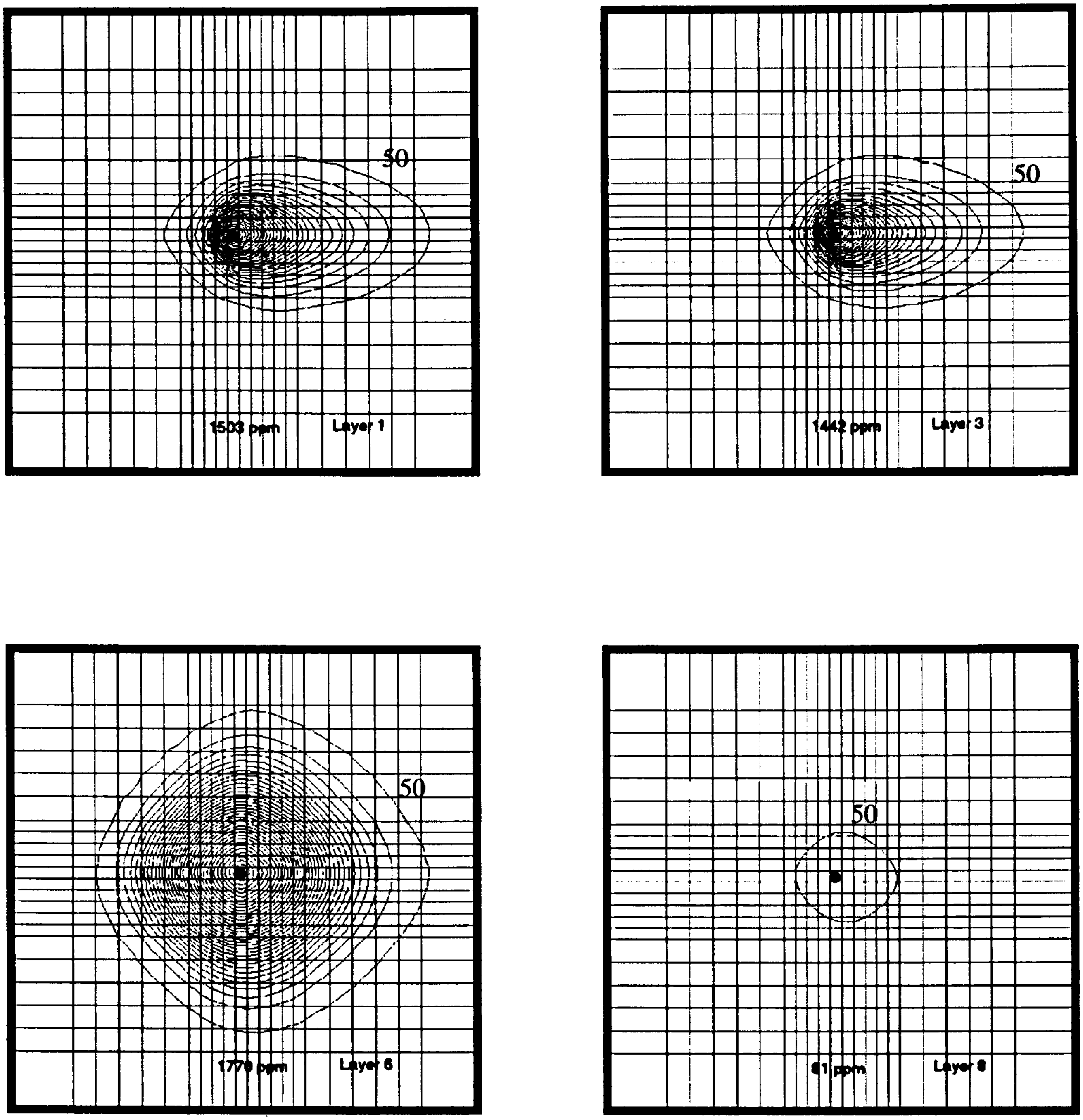

Figure 5.3 The computed concentrations of Case 3. The number in each plot is the maximum concentration. Contour interval = 50 ppm.

westward velocities are 0.03 m/day and - 0.03 m/day, respectively. Since the groundwater flow is eastward, the westward velocity of the saline water is reduced by the groundwater flow thereby limiting the westward spreading of the saline water as shown in Fig. 5.3. The injection fluxes on the north and south sides of the well are vertical to the groundwater flow direction, so basically the spreading on these two sides is symmetric. The isolines of solute concentration are symmetrical with respect to the longitudinal flow direction. In layer 6, the inflow rate is 150 m^3/day, so the eastward and westward velocities are 0.5 m/day and - 0.5 m/day. The westward velocity is much larger than the regional eastward flow of 0.017 m/day, thus westward spreading of the saline water is obvious substantial.

5.2.2 Multiple Well Source and Sink

The two-well system consists of an irrigation well and a municipal well. The interaction between these two wells is investigated. The model grid has 27 rows, and 43 columns (Fig. 5.2), and 8 layers meshed the same as for the single well cases except for different girding. The irrigation well is located in the area with the finer grid size and the municipal well is located 500 meters to the east. Four cases are considered and described in Table 5.3. The municipal well is screened in layers 7 and 8, and the pumpage is $2180\ m^3/\text{day}$ (~ 400 gpm) and is assumed to occur at a constant rate in every other month. The annular space between the borehole and the well casing is sealed in the municipal well. Cases 5-8 are same as Cases 1-4 except for the different location of the irrigation well and the addition of the municipal well. The maximum concentrations are

Table 5.3 Cases for multiple well simulation.

Case	Location of point source	Source strength	Total flowrate of saline water	Irrigation pumping	Municipal pumping
5	Layers 1-5 Layer 6	10 m^3/day each 150 m^3/day	200 m^3/day	no	2180 m^3/day every other month
6	Layers 1-5 Layer 6	20 m^3/day each 100 m^3/day	200 m^3/day	no	2180 m^3/day every other month
7	Layers 1-5 Layer 6	10 m^3/day each 150 m^3/day	200 m^3/day	4360 m^3/day in May., Jul., and Aug.	2180 m^3/day every other month
8	Layers 1-5 Layer 6	20 m^3/day each 100 m^3/day	200 m^3/day	4360 m^3/day in May., Jul., and Aug.	2180 m^3/day every other month

smaller than the single-well cases because they are affected by the municipal pumping which disperses the salinity more into the fresh part of the aquifer.

VI. FURTHER RESEARCH TO BE COMPLETED

Research will be conducted on the following two problems.

1. The conceptual model will include the leakage of the saline water in the upper aquifer to the Ogallala aquifer. Numerical solutions for a single well and multiple wells will be carried out for a simulation period longer than one year. The estimation of model parameters through an inverse approach using the geological structure method as described in Chapter IV will be conducted.

2. The methods proposed in Chapter IV will be applied to study the groundwater flow and solute transport in the Deerfield area shown in Fig. 6.1. Figure 6.2 shows the locations of well logs. The three water supply wells for Deerfield are shown in Fig. 6.1. The location of multi-level monitoring wells proposed by Kansas Geological Survey is also shown in the figure. Figure 6.3 shows the sulfate concentration for the well water supply. Measurements of sulfate concentration are available for water from wells 1 or 2 for 1949-1959 and wells 1, 2, or 3 for 1960-1976. The sulfate values for 1977 to 1993 are for water collected from the distribution system and represent a mixture of water pumped from the supply wells. Individual well records are not available for this period. Use of well 1 was discontinued after installation of well 4 in 1978 which has a larger yield. Starting in 1995, samples were collected from individual wells again; the sulfate concentration represents the average for wells 2, 3, and 4 during 1995-1997. Samples are now taken by the City once in every two years. The last data are for samples collected and analyzed by the Kansas Geological Survey in April 1997. The Survey will continue to collect samples from each well every few months for the next two years.

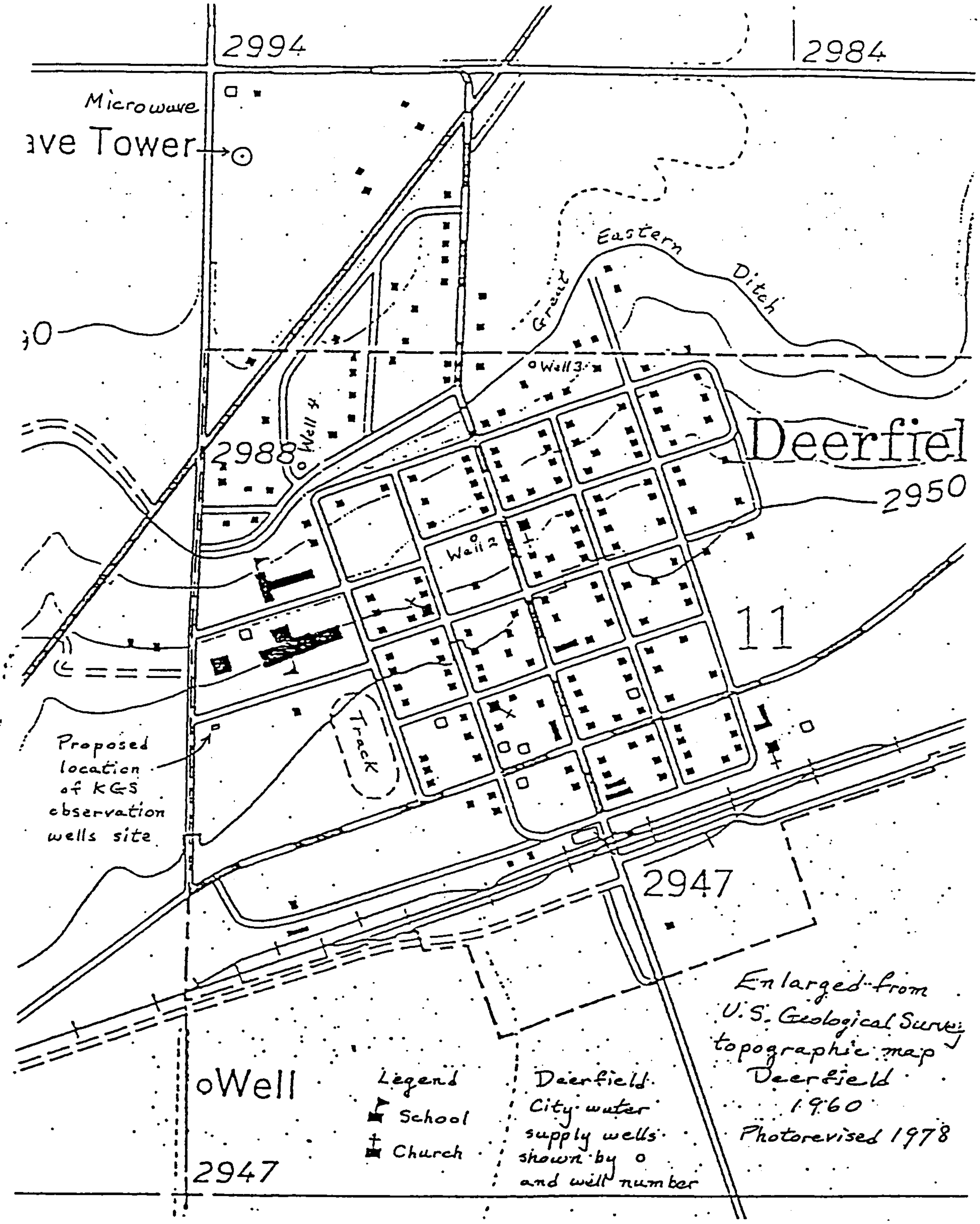

Figure 6.1 The Deerfield area.

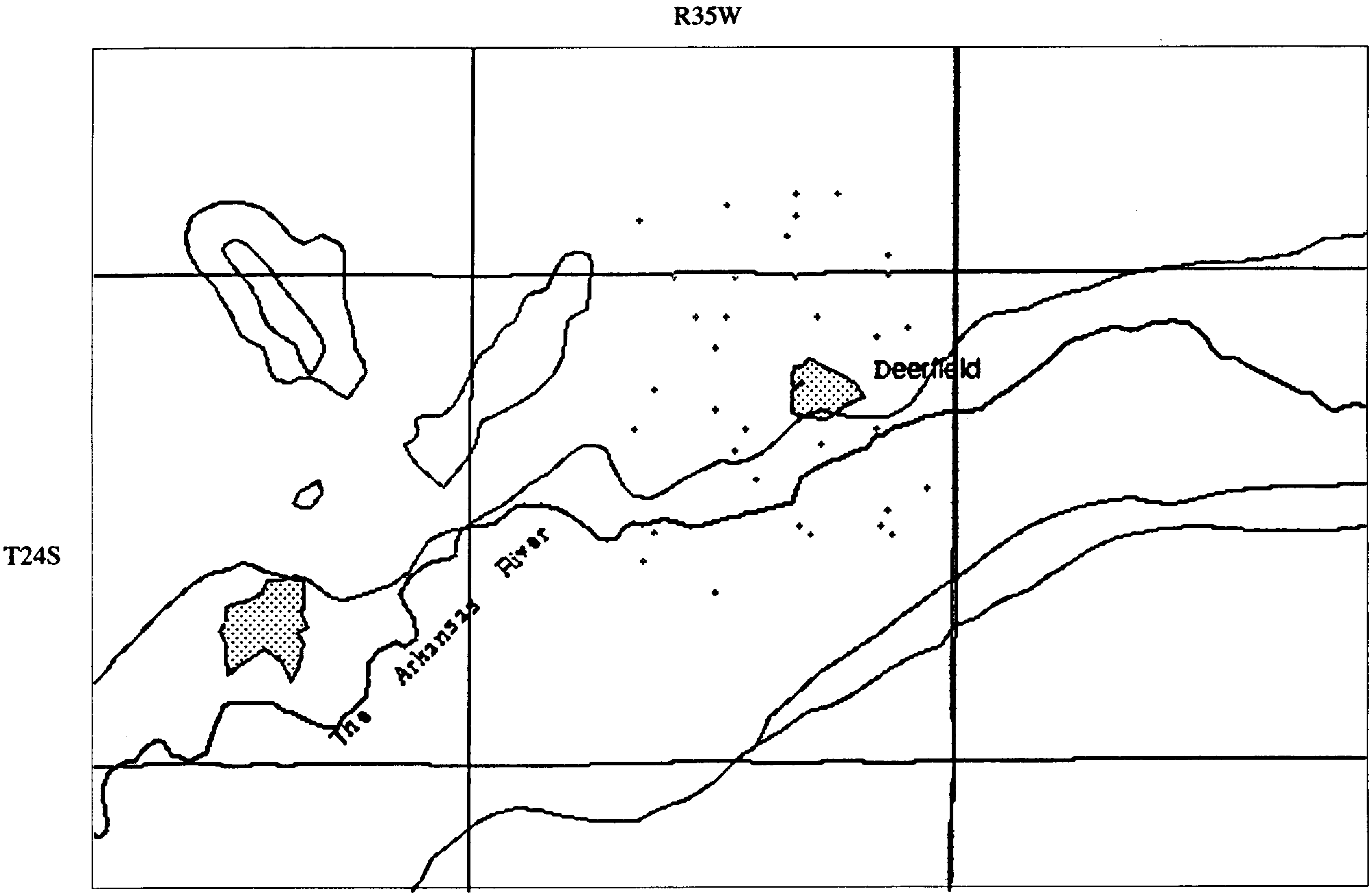

Figure 6.2 The locations of 36 well logs.

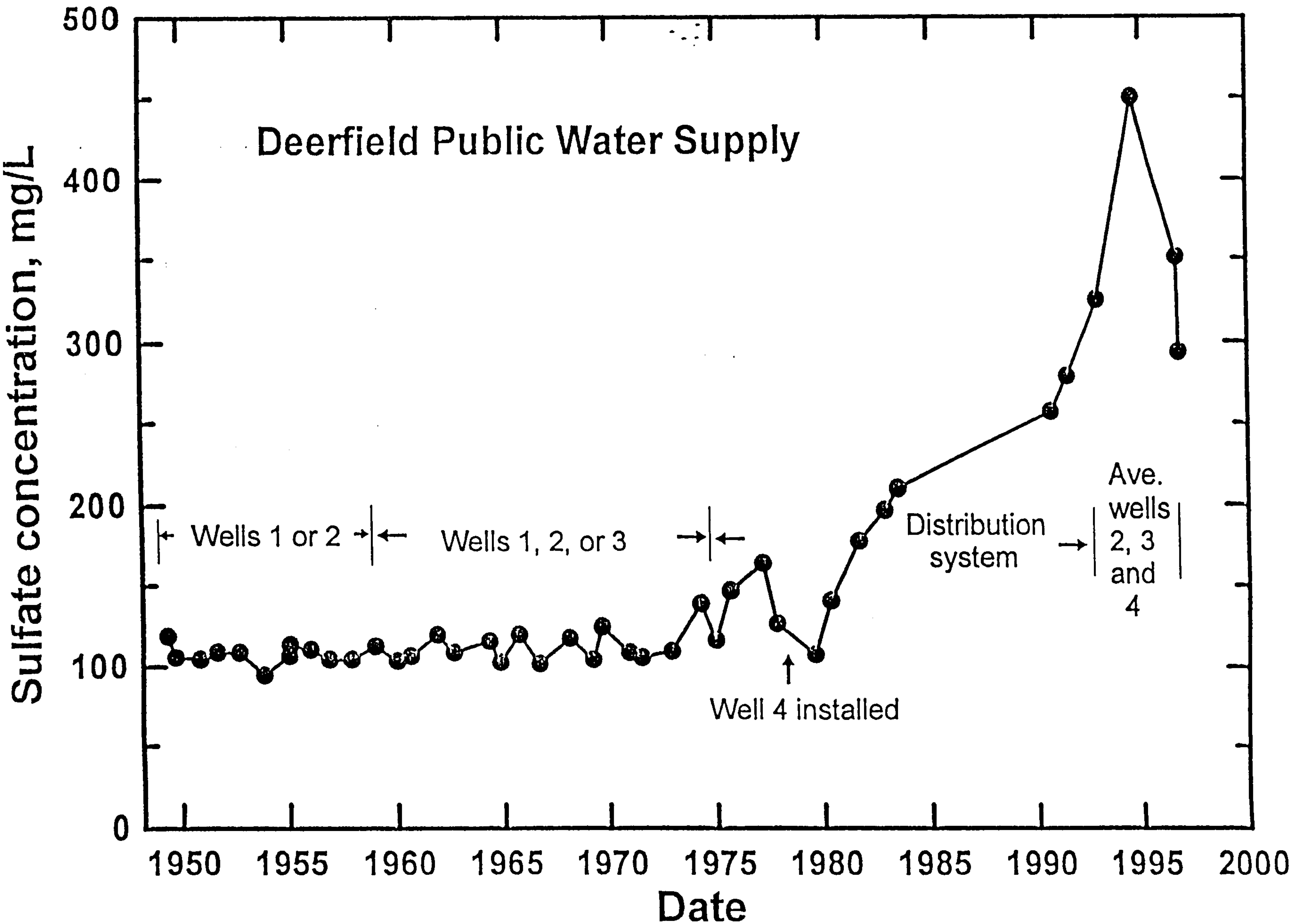

Figure 6.3. Observed sulfate concentration for Deerfield public water supply.

References

Ahlfeld, D. P. and Zafirakou, A., 1994. An algorithm for approximate solution of the groundwater contaminant remediation problem. Computational methods in water resources X, Kluwer Academic Publishers, Netherlands.

Bard, Y., 1974. Nonlinear parameter estimation. Academic Press, San Diego, California.

Blandford, T. N and Huyakorn, P. S., 1990. A modular semi-analytical model for the delineation of wellhead protection areas. U.S. Enviromental Protection Agency Office of Ground-Water Protection, Washington, DC.

Bureau of Reclamation, 1993. Arkansas River water management improvement study-Modeling of chloride transport in the Equus Beds aquifer. Technical report. U. S. Department of Interior.

Burrough, P. A., 1986. Principles of geographic information systems for land resources assessment. Clarendon Press, Oxford, Great Britain.

Cooley, R. J., 1979. A method of estimating parameters and assessing reliability for models of steady state groundwater flow: 2. Application of statistical analysis. Water Resources Research, v 15, no. 3, pp. 603-617.

Davis, J. C., 1986. Statistics and data analysis in geology, 2nd ed., John Wiley, New York.

Deutsch, C. and Journel, A., 1992. GSLIB: Geological software library and user's guide. Oxford University Press, New York.

DeVantier, B. A., and Feldman, A. D., 1993. Review of GIS applications in hydrologic modeling. Journal of Water Resources Planning and Management, v. 119, no. 2, pp. 229-245.

Doherty, J., 1994. PEST. Watermark Computing, Corinda, Australia.

Dunlap, L. E., Lindgren, R. J., and Sauer, C. G., 1985. Geohydrology and model analysis of the stream-aquifer system along the Arkansas River in Kearny and Finney counties. southwestern Kansas: U. S. Geological Survey, Water-supply Paper 2253, 52 p.

El-Kadi, A. I., Oloufa, A. A., Eltahan, A. A., and Malik, H. U., 1994. Use of a geographic information system in site-specific ground-water modeling. Ground Water, v. 32, no. 4, pp. 617-625.

Eppstein, M. J. and Dougherty, D. E., 1996. Simultaneous estimation of transmissivity values and zonation. Water Resources Research, v 32, no. 11, pp. 3321-3336.

Morehouse, S., 1992. The ARC/INFO geographic information system. Computer and Geoscience, v. 18, no. 4, pp 435-441.

Neuman, S. P., 1973. Calibration of distributed parameter groundwater flow models viewed as a multiple-objective decision process under uncertainty. Water Resources Research, v 9, no. 4, pp. 1006-1021.

Reeves, M., Ward, D. S., Johns, N. D., Cranwell, R. M., 1986. Theory and implementation for SWIFT II, the Sandia Water-Isolation Flow and Transport Model for Fractured Media. Rep. NUREG/CR-3328 and SAND83-1159, Sandia National Lab., Albuquerque, N. M.

Rifai, H. S., Hendricks, L. A., Kilborn, K., and Bedient, P. B., 1993. A geographic information system (GIS) user interface for delineating wellhead protection areas. Ground Water, v. 31, no. 3, pp. 480-488.

Roaza, H., Roaza, R. M., and Wagner, J. R., 1993. Integrating geographic information systems in ground-water applications using numerical modeling techniques. Water Resources Bulletin, v.29, no. 6, pp. 981-988.

Rushton, K. R. and Redshaw, S. C., 1979. Seepage and groundwater flow-numerical analysis by analog and digital methods. John Wiely and Sons, New York.

Strecker, E. W. and Chu, W., 1986. Parameter identification of a ground-water contaminant transport model. Ground Water, v. 24, pp. 56-62.

Sun, N. Z., 1994. Inverse problems in groundwater modeling. Kluwer Academic Publishers, Netherlands.

Sun, N. Z., Jeng, M. C., and Yeh, W., 1995. A proposed geological parameterization method for parameter identification in three-dimensional groundwater modeling. Water Resources Research, v. 31, no. 1, pp. 89-102.

Tsou, M.-S., and Whittemore, D. O., 1996. Interfacing Geographic information Systems with Groundwater models. EOS, Transactions, American Geophysical Union Fall Meeting, v. 77, no. 46, pp. 264.

Tim, U. S., Dharmesh, J., and Liao, H.-H., 1996. Interactive modeling of ground-water vulnerability within a geographic information system environment. Ground Water, v. 34, no. 4, pp. 618-627.

U.S.G.S. Water Resources Data Kansas Water Year 1995. U.S. Geological Survey Water-Data Report KS -95-1.

Wagner, B. J. and Gorelick, S. M., 1987. Optimal groundwater quality management under parameter uncertainty. Water Resources Research, v 23, no. 7, pp. 1162-1174.

Wagner, B. J., 1992. Simultaneous parameter estimation and contaminant source characterization for coupled groundwater flow and contaminant transport modelling. Journal of Hydrology, v. 135, pp. 275-303

Watkins, D. W., McKinney, D. C., Maidment, D. R., and Lin, M.-D., 1996. Use of geographic information systems in ground-water flow modeling. Journal of Water Resources Planning and Management, v. 122, no. 2, pp. 88-96.

Whittemore, D. O., Tsou, M.-S., and Grauer, J., 1996. Upper Arkansas River corridor study: Inventory of available data and development of conceptual models. Kansas Geological Survey Open-File Report 96-19.

Whittemore, D. O., and Butler, J.J., 1997. Invasion of saline water along the Arkansas River. 30th Annual Conference and Exhibition for Public Water and Wastewater Systems, Kansas Rural Water Association, Wichita, Kansas.

Xiang, Y., Sykes, J. F., and Thomson, N. R., 1992. A composite L_1 parameter estimation for model fitting in groundwater flow and solute transport simulation. Water Resources Research, v 29, no. 6, pp. 1661-1673.

Yeh, W., 1986. Review of parameter identification procedures in groundwater hydrology: the inverse problem. Water Resources Research, v 22, no. 2, pp. 95-108.

Yu, Y. S., 1991. Parameter identification in water resources. Proceedings, the Fourth International Conference on Computing Civil and Building Engineering, Tokyo, Japan, July 29-31, pp. 361-364.

Zheng, C., 1992. A modular three-dimensional transport model for simulation of advection, dispersion and chemical reactions of contaminants in groundwater systems. S. S. Papadopulos & Associates, Inc. Rockville, Maryland.